NATIONAL AERONAUTICS AND SPACE ADMINISTRATION

Technical Report 32-1495

Thermoelectric Generators for Deep Space Application

P. Rouklove
V. Truscello

JET PROPULSION LABORATORY
CALIFORNIA INSTITUTE OF TECHNOLOGY
PASADENA, CALIFORNIA

January 15, 1971

NATIONAL AERONAUTICS AND SPACE ADMINISTRATION

Technical Report 32-1495

Thermoelectric Generators for Deep Space Application

P. Rouklove
V. Truscello

JET PROPULSION LABORATORY
CALIFORNIA INSTITUTE OF TECHNOLOGY
PASADENA, CALIFORNIA

January 15, 1971

Prepared Under Contract No. NAS 7-100
National Aeronautics and Space Administration

Preface

The work described in this report was performed by the Guidance and Control Division of the Jet Propulsion Laboratory.

Acknowledgment

The authors are grateful to the following individuals for their assistance: G. Bodt, Dr. R. Campbell, M. Dore, R. F. Gruber, Dr. M. Reier, G. Stapfer, F. de Winter, and A. Zoltan.

Contents

I. Introduction 1

II. Power-Source Selection 2

III. Mission Requirements 2

IV. Spacecraft Interface 3

V. Science Payload Interface 3

VI. RTG Considerations and Selection 7

A. Materials 7

B. Generator Design Criteria 9

VII. Tests at JPL 11

VIII. Results of the Generator Tests 12

A. SNAP-11 Generators 12

B. SNAP-19 Generators 14

C. Integrated Heat-Pipe Tubular Module 18

D. SNAP-27 Generators 18

E. Module Tests 19

IX. Conclusions 19

Tables

1. Missions to the outer planets 4

2. Shielding requirements 8

3. Comparison of Z 9

4. Power requirements 10

5. Magnetic moment, SNAP-19 generator 21 14

Figures

1. Performance of solar panels and RTG in space 2

2. Spacecraft interfaces 5

3. Spacecraft iterations 6

Contents (contd)

Figures (contd)

4. Radial and axial radiation pattern vs time and distance 6
5. Axial radiation pattern, 8 ft from center 6
6. Generator test laboratory 12
7. Generator SNAP-11 in thermal vacuum 13
8. SNAP-11, power vs time 14
9. *Nimbus* spacecraft 15
10. SNAP-19, section view 16
11. Pb-Te couples, exploded view 16
12. SNAP-19, SN/21, power vs time 16
13. SNAP-19, SN/20, I-V characteristics 17
14. Fin root/power output dependence 17
15. SNAP-19, SN/20, cycling tests 17
16. Power input/power output 17
17. SNAP-19, SN/20, power vs time 18
18. Tubular thermoelectric generator 18
19. Tubular module, exploded view 18
20. Tubular module temperature profile 19
21. SNAP-27 in test chamber 19
22. SNAP-27 generator performance 19
23. Multielement modules, power vs time 20

Abstract

To provide a source of electrical energy independent of the sun, for the use of unmanned spacecraft investigation of the outer planets, the Jet Propulsion Laboratory (JPL) is evaluating radioisotope thermoelectric generators. Criteria for the selection of the thermoelectric materials, the design of the generator, and its integration with the spacecraft are discussed. Results of the tests of 10 generators that have been, or are presently, under test at JPL are also presented.

Thermoelectric Generators for Deep Space Application

I. Introduction

The scientific unmanned investigation of interplanetary space and of the outer planets requires a source of electrical energy independent of the sun. Of the several sources of power from which electrical energy can be obtained in space, only nuclear energy appears to be acceptable.

In all probability, a significant part of the space effort in the USA during the 1970 decade and beyond will be dedicated to manned earth satellites or lunar laboratories and to the unmanned exploration of the farthest planets of the solar system. This latter effort will be conducted with the assistance of space probes which are presently under development and which will rely on energy from nonsolar sources. Only long-life isotopes coupled with direct-energy-conversion techniques appear to provide the answer to the problems arising from long-term mission requirements, the probable mission environments, and the spacecraft limitations. Of the direct-energy-conversion techniques available, the radioisotope thermoelectric generator (RTG) appears to be the most promising candidate. The RTG has been under development since the late 1940s and has successfully demonstrated its capability to operate in earth-orbiting spacecrafts. However, the successful integration of such a device with the spacecraft, considering all of the mission requirements, presents severe problems of a mechanical, thermal, nuclear, magnetic, and electrical nature. Moreover, the reliability required to assure the successful execution of space missions lasting 12 years or more severely taxes the present technology.

The early realization of these problems motivated JPL, under the sponsorship of NASA, to initiate a program to evaluate the use of thermoelectric power for space application. This program was designed to obtain the necessary experience in the use of thermoelectric power generators and to provide the knowledge and understanding indispensable to the integration of an RTG into the spacecraft for the future space missions being considered by NASA.

II. Power-Source Selection

Three sources of energy are available for the production of electrical power in space. Two of these, solar and nuclear, are acceptable for long-term operation in space, while the third, chemical, cannot be considered for the continuous production of electricity over a 10-year period.

To date, solar-powered devices have found widespread application in many NASA space programs. Specific performance approaching 10 W/lb has been demonstrated on flight programs. Present developments in the field of lightweight large-area solar arrays (both fold-out and roll-up) indicate that the specific performance can be increased to 20–35 W/lb.

However, such performance is based on the power produced at earth (1 AU). As a spacecraft using solar panels moves toward the outer planets, the power-producing capability of the solar array will decrease due to the decrease in solar intensity and the degrading effects of particulate radiation (protons). Although the latter effect is only about 20% for a 10-year mission, the reduction in solar intensity will decrease the panel output by a factor of nearly 1000 at 30 AU. It is possible to define an effective specific performance (W/lb) based on the weight of a solar array necessary to produce a given amount of electrical power during encounter with each of the outer planets. Obviously, the specific performance at Jupiter (5 AU) will be higher than at the planet Neptune, which is at a distance of about 30 AU from the sun.

Figure 1 presents the variation of panel specific performance as a function of space-probe distance for both present-day (10 W/lb at 1 AU) and advanced solar-panel technology (20–30 W/lb). Note that at distances of 30 AU, a power system capable of producing 300 W(e) would have a specific performance of 0.01–0.035 W/lb and would weigh between 7500 and 30,000 lb. Thus, it is more than clear that even the most advanced solar-array concepts must be discarded for missions to the outer planets.

Having eliminated solar and chemical sources, one is left with the possibility of using some form of a nuclear device to supply electrical power for the outer-planet missions. A practical nuclear reactor for space application is still remote enough to be unavailable for missions to be executed between 1970 and 1980. And even if it were available, the cost considerations of launching such a

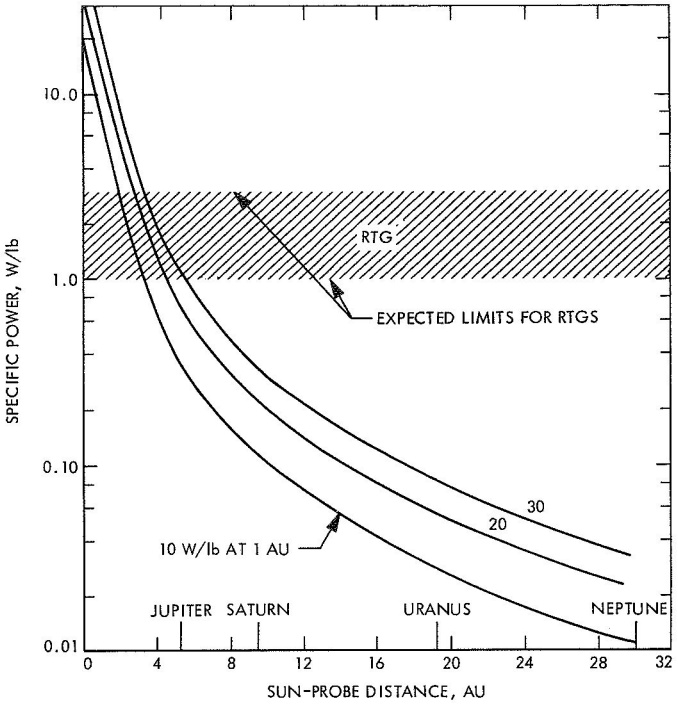

Fig. 1. Performance of solar panels and RTG in space

device are prohibitive except for very specific missions, such as large communication satellites or the manned exploration of the planets where relatively large amounts of electrical power are necessary.

Devices using isotope decay as the energy source, coupled with some form of static energy conversion, appear to be the most attractive candidates. The other forms of nuclear energy conversion available or under development, namely, the dynamic systems based on the different thermodynamic cycles, are considered impractical for deep-space probes because of excessive weight at the low electrical-power requirements, long-term operation reliability, and stage of development. The two static devices available for converting isotopic energy are (1) the radioisotope thermionic generator and (2) the radioisotope thermoelectric generator (RTG). Of these, the latter, which is in a more advanced stage of development, and as previously mentioned, has already successfully demonstrated its capability of operation in space, is the choice of the spacecraft designer.

III. Mission Requirements

The time and duration of the mission, the power profile, the direction of the mission, and the scientific goals

of the mission have strong influences on the RTG, the spacecraft design, and the subsequent interface between the two. Some of the missions to the outer planets considered in the 1970 decade are presented in Table 1. Power requirements for these missions range from 300 to 500 W(e), while mission duration can extend to 12 years. The length of these missions and the hardship to which the spacecraft will be exposed severely tax the reliability of all spacecraft components and the present space technology. For instance, the long duration of the mission will require developments in electronics to include redundancy, self test and repair capability, and radiation hardening. The hazards of meteorite encounters and the obstacle presented by the rings of Saturn may require a substantial increase in the weight of the spacecraft to provide proper shielding, or could increase the duration of the mission by as much as 2 years to evade these obstacles. The alternative of passing between the Saturnian atmosphere and the inner ring offers considerable risk of catastrophic impact. The duration of the mission not only poses problems of reliability but also of communications. Round-trip signal-transmission times of up to 8 h or more are necessary. To achieve effective communications with a plausible transmission power, large antennas accurately oriented toward earth are required. The presence and size of such antennas (16 ft in diameter or more) have a strong influence on the spacecraft design and on the location and design of the RTG to avoid thermal and radio interferences. The duration and goals of the mission also severely tax the attitude control and the propulsion systems for spacecraft trajectory correction. (These systems are used during the cruise or during the insertion maneuvers into the planetary orbits.)

IV. Spacecraft Interface

The decision to utilize an RTG as the power source introduces a completely new and different spectrum of problems to the spacecraft designer. Beyond the normal spacecraft interfaces, such as weight limitations and booster-fairing-shroud constraints, the presence of the RTG on the spacecraft creates problems related to the nuclear radiation interference with the spacecraft components, thermal interface problems, and mechanical problems related to boom deployment and stowage, and the location of the center of mass. The RTG is one of the heaviest components of the spacecraft and its location must be carefully analyzed. To avoid excessive thermal and radiation interference without the use of extensive shielding, the RTG is generally located on a boom which is deployed during the flight. This, however, has a marked influence on the moments of inertia of the spacecraft, and hence directly influences attitude control. The incorporation and design of the boom, its optimum length, methods of attachment to the spacecraft, and the deployment mechanisms, all strongly influence the spacecraft configuration and must be considered at an early stage of the design. The alternative of locating the RTG on or near the spacecraft body increases the thermal and nuclear radiation problems and requires serious increases in weight. The location of the RTG may be further influenced by such considerations as possible damage by exposure to the plumes from the correction rockets. Some of the interfaces considered during the spacecraft iterative designs and three of the spacecraft iterations considered for an Earth-Jupiter-Neptune mission are presented in Figs. 2 and 3.

V. Science Payload Interface

Since the primary objectives of a deep-space probe are the measurement of ambient particles and fields, the investigation of planetary atmospheres, and the possible visual observation of the planets, the scientific payload considerations take priority in the design of a spacecraft. Following is a list of possible experiments to be installed on a spacecraft for an Earth-Jupiter-Saturn-Uranus-Neptune mission using planetary gravity assist:

(1) Micrometeorite detector.

(2) Infrared radiometer.

(3) Infrared interferometer.

(4) Ultraviolet photometer.

(5) Trapped radiation detector.

(6) Cosmic dust detector.

(7) DC magnetometer.

(8) Charged particle telescope.

(9) Plasma probe.

(10) Low energy proton and electron differential analyzer.

(11) Cosmic ray telescope.

(12) Television.

Some of these experiments are insensitive to the presence of the RTG; others, especially those designed to measure

Table 1. Missions to the outer planets

Characteristics	Jupiter, Saturn interior ring, Uranus, Neptune		Jupiter, Saturn exterior ring, Uranus, Neptune		Jupiter, Uranus, Neptune		Jupiter, Pluto	Saturn (direct)	Uranus (direct)	Neptune (direct)	Pluto (direct)
	1976	1977	1977	1978	1978	1979	1977	1979	1977, 1978	1977	1976
Launch period, days	15	15	15	15	15	15	15	15	15	15	15
Maximum launch energy required, km^2/s^2	104	120	100	108	110	110	110	140	139	150	180
Capability for Titan III/Centaur (spacecraft weight; 114-deg azimuth), lb[a]	1400	780	1530	1250	1190	1190	1190	140	150	0	—
Capability for Titan III/Centaur Burner II 1440 (spacecraft weight; 114-deg azimuth), lb[a]	1700	1380	1800	1620	1580	1580	1580	900	930	700	—
Maximum declination at launch (absolute value), deg	14	27	33	33	32	27	28	37	7	4	26
Jupiter encounter											
Flight time from launch, days	561	511	652	593	564	579	551				
Flyby altitude, km	16,000	212,000	622,000	1,600,000	62,000	560,000	236,000	—	—	—	—
(Jupiter surface radius)	(0.2)	(3.0)	(8.8)	(22.5)	(0.9)	(7.8)	(3.3)				
Communication distance, 10^6 km	675	638	900	767	719	749	673				
Saturn encounter											
Flight time from launch,	1363	1095	1394	1240				1255			
days (yr)	(3.7)	(3.0)	(3.8)	(3.4)				(3.4)			
Flyby altitude, km	8,000	6,000	75,000	80,000	—	—	—	Open	—	—	—
(Saturn surface radius)	(0.1)	(0.1)	(1.2)	(1.3)				1310			
Communication distance, 10^6 km	1277	1562	1453	1321							
Uranus encounter											
Flight time from launch,	2798	2342	2945	2764	2293	2286			3092		
days (yr)	(7.7)	(6.4)	(8.1)	(7.6)	(6.6)	(6.3)			(8.5)		
Flyby altitude, km	32,000	16,000	86,000	121,000	22,000	41,000	—	—	Open	—	—
(Uranus surface radius)	(1.3)	(0.7)	(3.8)	(5.1)	(0.9)	(1.7)			2709		
Communication distance, 10^6 km	2781	2910	2900	2717	2972	2833					
Neptune encounter											
Flight time from launch,	3894	3372	4100	4030	3503	3599				6209	
days (yr)	(10.7)	(9.2)	(11.2)	(11.0)	(9.6)	(9.9)				(17.0)	
Flyby altitude, km	Open	Open	Open	Open	Open	Open	—	—	—	Open	—
Communication distance, 10^6 km	4519	4613	4587	4642	4440	4457				4659	
Pluto encounter											
Flight time from launch, days (yr)	—	—	—	—	—	—	3500 (9.6)	—	—	—	15,231 (41.7)
Flyby altitude, km							Open				Open
Communication distance, 10^6 km							3919				4934

[a] J. Long, private communication.

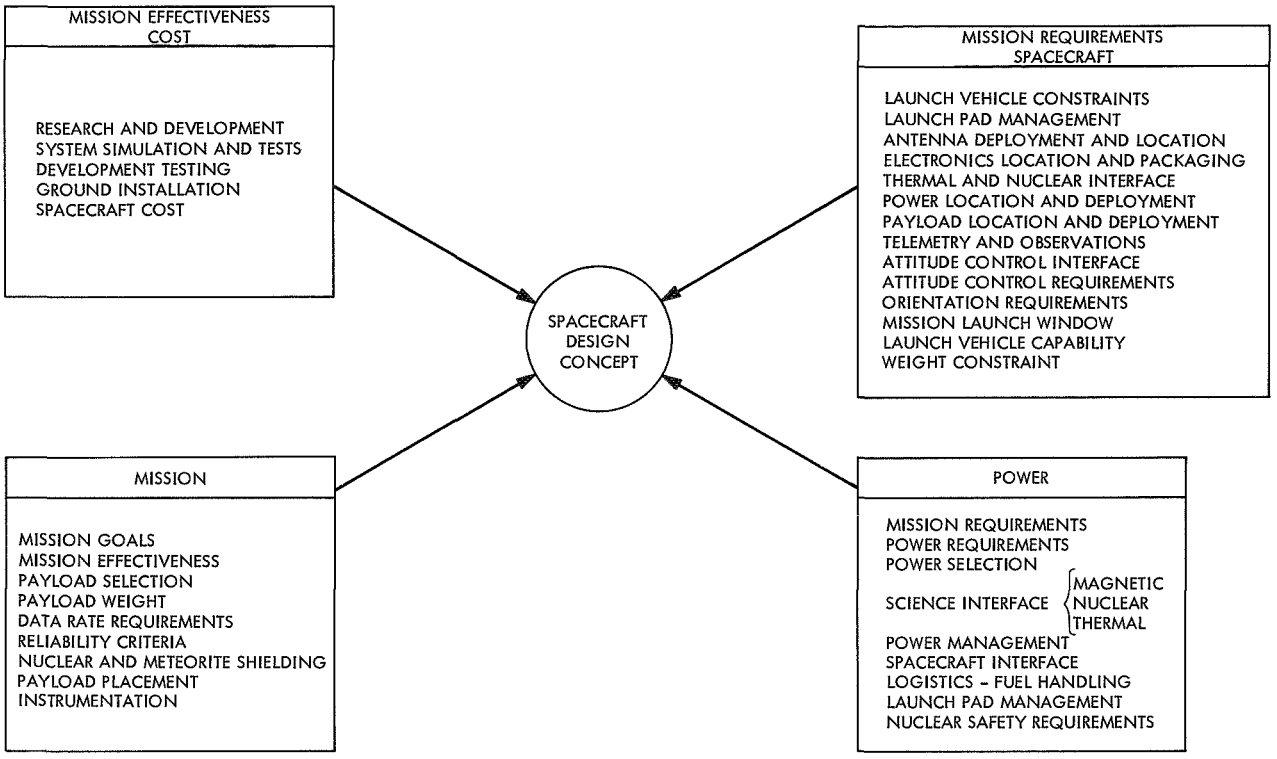

Fig. 2. Spacecraft interfaces

the planetary and interplanetary charged-particle radiations and the magnetic fields, can be seriously affected by the gamma, neutron, or magnetic radiations from the RTG. Also, some of the infrared sensors can be disturbed by the thermal background resulting from the RTG. The gamma radiation pattern from an RTG configuration using Pu-238 as the energy source is presented in Figs. 4 and 5. It is clear that, due to self-shielding effects, a preferred generator orientation exists, resulting in a minimum-shielding requirement. Moreover, the recognition of such a pattern strongly influences the spacecraft design. RTGs have been integrated on several spacecraft including *Transit* and *Nimbus*. However, none of these satellites contained scientific experiments very sensitive to the radiation and magnetic fields. The unsuccessful attempt to integrate an RTG with a predesigned satellite carrying radiation-sensitive experiments (the *IMP* satellite) exemplifies the necessity of a careful RTG integration process in the design of a spacecraft.

The nuclear radiations and magnetic interactions between the spacecraft and the RTG can be divided into three broad categories: (1) radiation damage to the electronic components, (2) interference with the measurements of the interplanetary radiation fields, and (3) perturbation in the measurements of the interplanetary magnetic fields. Of a lesser importance are the thermal effects on some of the scientific experiments.

Radiation damage to the electronic equipment can be minimized by the proper selection of radiation-hardened components and design of electrical circuits to accommodate changes in operational characteristics due to radiation effects. Locating the spacecraft subsystems so that the various components will not be exposed to radiation levels above 10^{10} neutrons/cm^2 and 10^5 rad of gamma radiation will also help minimize radiation damage. In principle, shielding can be used to reduce the radiation levels. Generally, however, shielding to reduce neutron levels, which are the main contributors to permanent radiation damage, carries a larger weight penalty than is justified by the resulting decrease in flux. An alternative to shielding for neutrons would be to remove some of the impurities in the heat source.

The numerous studies conducted at JPL indicate that permanent damage effects on electronic components and spacecraft subsystems are, at worst, marginal for certain sensitive components and are negligible for the majority of the components. Of more concern is the problem of

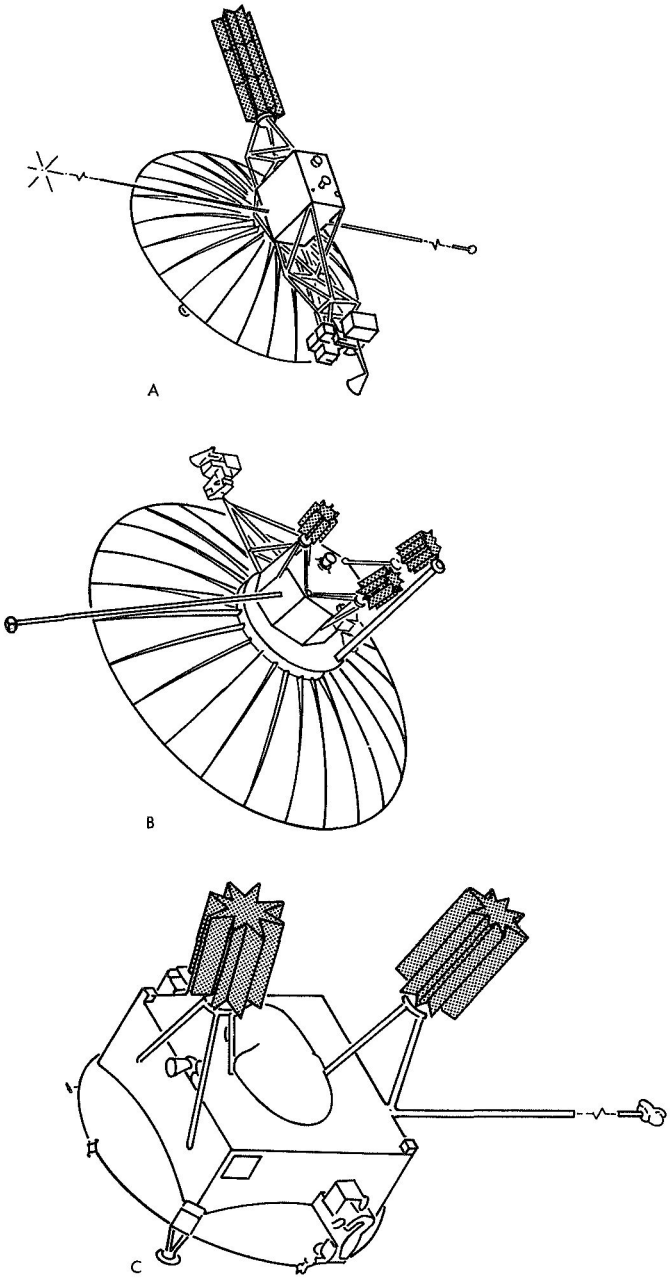

Fig. 3. Spacecraft iterations

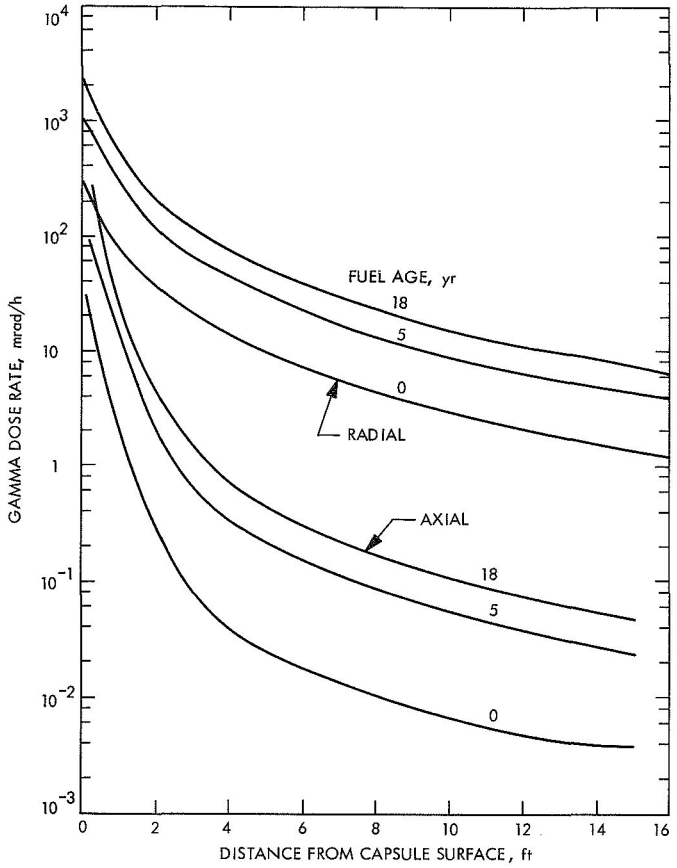

Fig. 4. Radial and axial radiation pattern vs time and distance

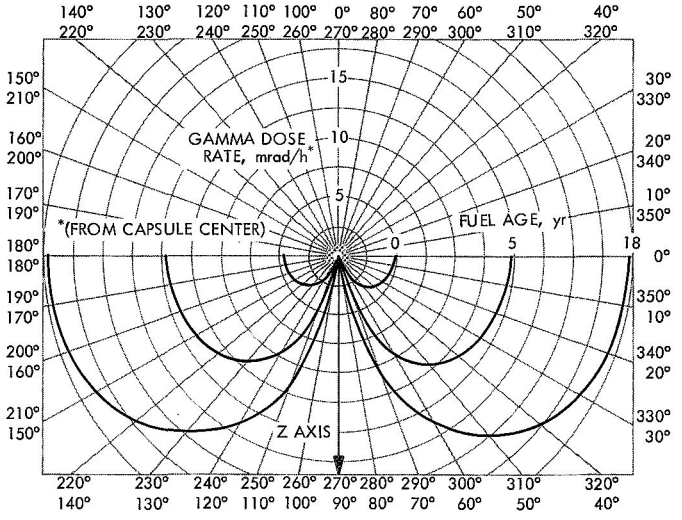

Fig. 5. Axial radiation pattern, 8 ft from center

operating scientific instruments in the RTG environment which are susceptible to energetic radiation. Elements of an optical train may darken upon exposure to gamma radiation, or pulses due to gamma or neutron radiation from the RTG may be difficult to distinguish from those caused by the external particle flux. Examples of susceptible detectors are scintillation devices, surface-barrier solid state devices, and ionization chambers.

In practice, most of the instruments for scientific experiments do not depend on particle ionization or emission for proper functioning. Equally important is the fact that many of the experiments concern themselves with electromagnetic radiation at wavelengths quite different from those caused by an RTG, or are designed to measure phenomena completely unrelated to the RTG-produced fields. Preliminary studies conducted at JPL indicate that probably the most critical instruments in the list of possible scientific experiments are the charged particle detectors.

The interference problems with these instruments can be minimized or circumvented to a large extent by (1) use of coincidence-counting techniques, such as those used in the cosmic-ray experiments on *Pioneer VI* and VII, (2) the judicious selection of the detector components within the instrument to minimize sensitivity, (3) separation of the sensitive components from the RTG through the use of extended booms, and (4) properly selected individual shielding techniques.

Studies at JPL have shown that separation distances of 15 ft coupled with a relatively small amount of shadow shielding located near a sensitive detector can reduce the radiation-interference effects to a tolerable level. Interestingly enough, placing the shield at the RTG greatly increases the shield weight requirements. Results of a radiation study for a typical complement of scientific instruments in a number of spacecraft configurations are shown in Table 2. The total shield requirements vary between 6 and 12 lb, depending on the spacecraft configuration, location of the RTGs relative to the science equipment, and the amount of self-shielding provided by the RTGs. The spacecraft configurations studied are given in Fig. 3.

The magnetic-field interaction results from two causes: the use of ferromagnetic materials in the construction of some of the devices and the relatively large current flow. The latter effect may be controlled by careful balancing of the current-carrying circuits and by appropriate location of degaussing loops. The use of magnetic materials in the generator assembly, however, creates problems of remanent fields and enhanced stray fields. This is more of a problem in the Pb-Te generators than in the generator assembled with Si-Ge material. This is illustrated by the magnetic fields measured on the SNAP-27 generator (12.5 gamma at 10 ft), and on the SNAPOODLE (0.25 gamma at 10 ft). The latter was assembled with Si-Ge thermoelectric elements. The magnetic field effects can also be attenuated by physical separation, the effect being roughly proportional to the inverse cube of the distance. For these reasons, the RTG and the scientific instruments should be separated as much as possible, i.e., on extended booms. This again has a strong influence on the spacecraft design.

VI. RTG Considerations and Selection

A. Materials

A convenient engineering-evaluation factor for thermoelectric materials is its figure-of-merit Z which contains the major physical properties of the materials: the Seebeck coefficient α (MV/°C), the electrical resistivity ρ (Ω/cm), and the coefficient of thermal conductivity K (W/cm°C) in the following relation:

$$Z = \frac{\alpha^2}{\rho_K} \ (1/°C)$$

The comparison of Z for a given ΔT for some of the most common thermoelectric materials is presented in Table 3. In commercial application, three basic materials are utilized: the bismuth telluride alloys (Bi-Te), the lead-telluride alloys (Pb-Te), and the silicon germanium alloys (Si-Ge). The Bi-Te alloys are used at low operating temperatures in terrestrial and underwater applications, while the Pb-Te and Si-Ge alloys are used for space applications. All the USA-flown radioisotope thermoelectric generators, namely, SNAP-3, 9A, 19, and 27, were assembled with Pb-Te or Pb-Sn-Te thermoelectric elements. The SNAP-10A (a small thermoelectric-reactor system) used Si-Ge thermoelectric couples to produce more than 400 electrical watts in space. Both the Pb-Te and Si-Ge compositions are semiconductors leaning toward metals rather than insulators. It is customary to designate the vacancy donor leg as the *P* element, while the electron donor element is designated as the *N* element. In the lead-telluride thermoelements, generally obtained by

Table 2. Shielding requirements (all values are for 18-year-old fuel)

Experiment	Detector	Sensitive Area, cm^2	Maximum allowable spurious counts/s	Flat shield area, cm	Shield thickness, in.			Flat shield weight, g			Shield weight per experiment, g		
					Configuration			Configuration			Configuration		
					A	B	C	A	B	C	A	B	C
Low energy proton and electron differential analyzer	Channeltron CEM-4010	2.01	0.1	6.0	2.17	2.77	3.68	562	718	953	789	1050	1430
	Geiger EON-6213	0.95	0.3	4.0	1.32	1.92	2.76	227	331	477	789	1050	1430
UV Photometer	Channeltron CEM-4010	2.01	0.1	10.0	2.17	2.77	3.68	936	1198	1588	1163	1529	2065
	Geiger EON-6213	0.95	0.3	4.0	1.32	1.92	2.76	227	331	477	1163	1529	2065
Trapped radiation detector	Solid state 12 $mm^2 \times 31\ \mu$	0.73	0.001	3.0	1.45	2.31	3.13	187	299	405	529	796	1121
	Geiger EON-6213	0.95	0.3	2.0 Each	1.32	1.92	2.76	341	497	715	529	796	1121
Cosmic ray telescope	Solid state 5.7 $cm^2 \times 200\ \mu$	8.48	1.0	10.0	0.33	1.25	1.98	141	540	855	141	540	855
Total shield weight, g											2624 (5.78 lb)	3917 (8.63 lb)	5472 (12.06 lb)

Table 3. Comparison of Z

Material	ΔT, °C	Maximum Temperature, °C	Average Z, $°C^{-1}$	Z × ΔT
Bi-Te	100	250	0.0018	0.18
Pb-Te	450	600	0.001	0.45
Zn-Sb	250	400	0.001	0.25
Ge-Bi-Te	450	600	0.001	0.45
Si-Ge	850	1000	0.0006	0.51
Pb-Sn-Te	400	550	0.001	0.40
Ag-Sb-Te	450	600	0.0015	0.68
Ce-S	1050	1200	0.0002	0.21

powder metallurgy or casting techniques, the *P* element has an excess telluride composition doped with sodium, while the electron donor *N* leg is of an excess lead composition doped with lead iodine. The early generators utilized TEGS 2N and TEGS 2P Pb-Te thermoelectric materials. Recently, however, a lead-tin-telluride composition doped with sodium and manganese (TEGS 3P), a lead-silver-selenium material, and a material containing Pb, Ag, Te, and Ge-Te and known as TAGS-85, also have become available. In the Pb-Te alloy family, the *N* element seldom causes failures at operating conditions. Most of the problems are caused by the more brittle *P* elements. The new materials previously mentioned are of the *P* type and, although in some cases lead to lower efficiencies, produce a stronger element, much less prone to electrical degradation. The degradation in the Pb-Te material is generally caused by the selective loss of materials (tellurium at the hot junction and redistribution of sodium), or by the loss of manganese by oxidation or precipitation in the Pb-Sn-Te-type material. The major reason for the degradation in 2P material is traced to reactions between the iron used at the hot shoe and the tellurium. These reactions generally lead to changes in the Seebeck coefficient and an increase in the electrical resistivity. At operating temperatures, the Pb-Te materials are readily oxidized in the presence of oxygen and sublime in vacuum; thus Pb-Te thermocouples must be operated in sealed containers under an inert atmosphere.

Although the lead-telluride materials provide more attractive conversion efficiencies at lower temperatures, they are more brittle and have lower tensile and shear strength than the Si-Ge compounds. As a result, the Pb-Te materials can support the launch and flight stresses only through the use of large compressive pressures provided by bulky and complex spring-and-piston mechanisms.

The silicon-germanium (Si-Ge) materials used at present consist of an approximate 70%-silicon/30%-germanium alloy doped to saturation with boron in the *P* leg and phosphorus in the *N* leg (approximately 10^{20} carrier/cm^3). In general, the Si-Ge material presents fewer problems. The material is stable in oxygen and in vacuum at operating temperature (vapor pressure at 800°C, approximately 3×10^{-9} torr). Its coefficient of expansion is 3.6 times lower than that of the Pb-Te (5×10^{-6}/°C vs 18×10^{-6}/°C); its tensile strength is approximately 5 times better than that of the Pb-Te (≈5000 psi vs 1000 psi), and the compressive strength is much higher (150,000 psi vs ~10,000 psi for the Pb-Te). The improved mechanical properties and lower density (3.5 g/cc as opposed to 8.3 g/cc for the Pb-Te) of the Si-Ge alloys have the advantage of a lower inertia to dynamic shocks (successfully tested up to 1000 g at JPL). Finally, the hot-shoe material and the bond problems which present difficulties in the Pb-Te case have successfully been resolved for the Si-Ge materials. The Si-Ge couples can operate cantilevered from the hot end, thus not requiring a complex and heavy spring-and-piston system at their cold end. However, the radiative-type thermal transfer, which has been adopted between the heat source and the thermopile, limits the module packing density and penalizes the fuel-capsule design by the requirement for higher surface temperatures.

In the Si-Ge thermocouples, the degradation in performance occurs on the *N* side as a consequence of the localized dopant precipitation, which results in a change in the thermoelectric characteristics (an increase in the Seebeck coefficient and electrical resistivity). However, this phenomenon is well understood and can be minimized by an optimum selection of the area ratio between the *N* and *P* elements during the design of the thermopile.

B. Generator Design Criteria

The design of a generator for space application, and especially for long-term missions, requires the consideration of many factors; among them: weight, efficiency, and reliability. Closely related with the last is the fact that the generator performance changes with time due to the decrease in fuel inventory and thermoelectric material degradation. To obtain maximum performance, the generator design is optimized for end-of-life (EOL) or end-of-mission (EOM) conditions; that is, the thermoelectrics are sized to convert the available heat to electricity

most efficiently at the end of the mission. This approach generally results in an excess power at the beginning of the mission because of greater fuel inventory and superior thermoelectric properties. This excess power, however, can be easily minimized and handled with the application of adequate design criteria and the use of shunt regulation.

The decrease in fuel inventory as a result of the normal isotope decay with the resultant generator-power decrease is predictable; however, the changes in the thermoelectric materials resulting from metallurgical or chemical reactions are much more difficult to evaluate due to lack of long-term (more than 10 years) test data. Changes are generally found to be more severe and less predictable in the generators assembled with Pb-Te alloys than in those using Si-Ge. These changes are strongly related to the operating temperatures, the environment surrounding the elements, and to the different transient mechanisms (thermal cycles, transient changes in the load, mechanical stresses, etc.), to which the elements are exposed. The insulation surrounding the thermoelectric couples has a very strong influence on the efficiency of the generator by reducing the thermal shunt losses. Up to a 30% gain in efficiency can be achieved by a judicious selection of the proper material (Dynaquartz, Min K, foil, etc.).

The high-reliability requirements are expected to be met by the use of several generators electrically interconnected in a parallel circuit and by the series-parallel interconnection of the couples and of the multicouple modules within the generator.

The outer-planet-spacecraft design presently being studied at JPL has a requirement of approximately 550 electrical watts at BOL (Table 4). Design studies indicate that this could be best achieved by providing 3 or 4 generators located in tandem on an extendable boom. This attachment system has several advantages: The judicious orientation of each generator will assist in the reduction of the stray magnetic field by cancellation. The self-shielding effect of the generators will reduce the radiation in the axial direction, which in turn is aligned with the sensitive components. Finally, the separation of the generators from the spacecraft, and from the remaining electronics on-board the spacecraft, will alleviate most of the thermal problems and increase the reliability of the electronic components. In the spacecraft configurations developed to date, the magnetometers and the RTGs are separated by 10 m for minimum interference. In the RTG design being considered, the couple geometry is being optimized for maximum performance at EOM (10 to 12 yr). The couples are interconnected—3 rows in parallel in each module, with the modules connected in series in

Table 4. Power requirements (estimated)[a]

Event/User	Power, W						
	Acquisition	Cruise	Midcourse maneuver	Midcourse burn	Encounter	Occultation	Playback
Science	43	43	43	0	80	50	43
Data acquisition	60	60	60	60	60	60	60
Transmission	65	75	75	65	80	130	65
Guidance/control	75	72	93	125	140	85	72
Power switch	5	5	5	5	5	5	5
Thermal control	25	25	25	25	25	25	25
Total demand	273	280	301	280	390	355	270
Contingency 25%	341	350	376	350	487	444	337
RTG Power (BOL) (90% conversion efficiency)	381	385	413	385	535	488	375

[a]Spacecraft weight, 310 kg
Ratio, power to science, 5.7
Ratio, spacecraft to power, 2.47
Ratio, spacecraft to science, 7

each generator to deliver 28 to 30 V. The wires interconnecting the modules will be routed to minimize the stray magnetic field by cancellation. Bucking coils will also be provided. The use of this interconnecting arrangement, the exclusive use of nonmagnetic materials in the construction of the generator, the low currents associated with the high voltage output, and the use of coaxial connections between generators and the power-conditioning equipment, will easily reduce the magnetic interference to a value smaller than 0.1 gamma at 10 m from the magnetometers (value required by the scientific experiments).

No long-term data (10 yr or more) is presently available on the behavior of generators during extended missions, but extrapolation of the large amount of data available for shorter periods of test (approximately 5 yr) indicates that a 25% total decrease in the power output may be expected, including that resulting from the decay of the radioisotope. Thus, the power output of such an array of generators at the beginning of life may be expected to be about 550 W. However, this number can be reduced by proper power-flattening design techniques, to a value nearly equal to the value required at EOM. The weight of the total power system, based on a specific weight of individual generators of 150 to 225 g/W, can be assumed to be between 126 and 85 kg, including power conditioning and nuclear shielding.

VII. Tests at JPL

The test program initiated at JPL for the evaluation of RTGs covers multiple phases: (1) tests of thermoelectric generators, (2) tests of multicouple thermoelectric modules, (3) tests of single-couple elements, (4) tests of fuel capsules to define the radiation dose rates and energy distribution, (5) tests of various scientific instruments to determine their sensitivity to radiation and to evaluate the shielding requirements, and (6) flight-approval tests of fueled generators integrated with the spacecraft. The tests are designed to supply accurate performance data on the state of the art of the generators and to provide the knowledge and understanding necessary to successfully integrate an RTG with the spacecraft. The test phase discussed herein covers only the testing of multicouple thermoelectric modules and complete generators which are heated with electrical heaters to simulate the isotope-fueled capsules.

A total of 10 generators have been or are under evaluation at the JPL Thermoelectric Laboratory. Figure 6 presents a view of one of the facilities in which four RTG units are under test, one in thermal vacuum environment and the others in ambient. Tests are also conducted in two other facilities while the work on fueled generators and the evaluation of the radiation on scientific instruments are carried on in an especially designed radiation facility.

The generator tests consist of extensive parametric evaluations, long-term life tests, and special tests to evaluate the generator behavior in simulated mission conditions. For economic reasons, the tests are performed whenever possible in ambient conditions. Normal air-convection cooling is used and insulation is selectively applied on the radiation fins and the generator body to obtain the nominal operating conditions. The generators are evaluated at three levels of power input: beginning-of-life (BOL), end-of-life (EOL), and at the maximum power input compatible with the construction limitations of the generator. The life tests are performed at the BOL input conditions and at the voltage output corresponding to the maximum power output. The parametric tests are performed for each level of power input at several selected values of voltage output. Special tests simulating changes in fuel inventory, environmental conditions and power requirements during the mission, and the effects of prelaunch and launch environments are also performed. The generators are moreover evaluated for resistance to acceleration, shock, and vibration at levels expected during the mission, and are also tested for magnetic moments and RF interference.

The test equipment used allows complete automation of the tests. All data are displayed, for greater accuracy, on digital voltmeters and are recorded on an hourly basis or on command on automatic data-recording equipment. The power input to the electrical heaters, used to simulate the isotope capsules, is controlled by an SCR-type proportional controller. This allows the input power to be maintained to within ± 1 W, or the hot junction temperature to within $\pm 1°C$. The generator's electrical output load consists of a solid-state circuitry capable of maintaining a selected voltage or current output from the generator to within ± 1 mV or 1 mA. Protective circuits are provided to prevent overheating of the generator or thermal shock as a result of loss of power input.

The thermal vacuum tests are performed in a 5 × 6-ft vacuum chamber provided with thermal shrouds. The temperature of the shrouds can be controlled and maintained at the desired value within $\pm 2°C$ from $-160°C$ to $+150°C$. The entire system is automatically operated

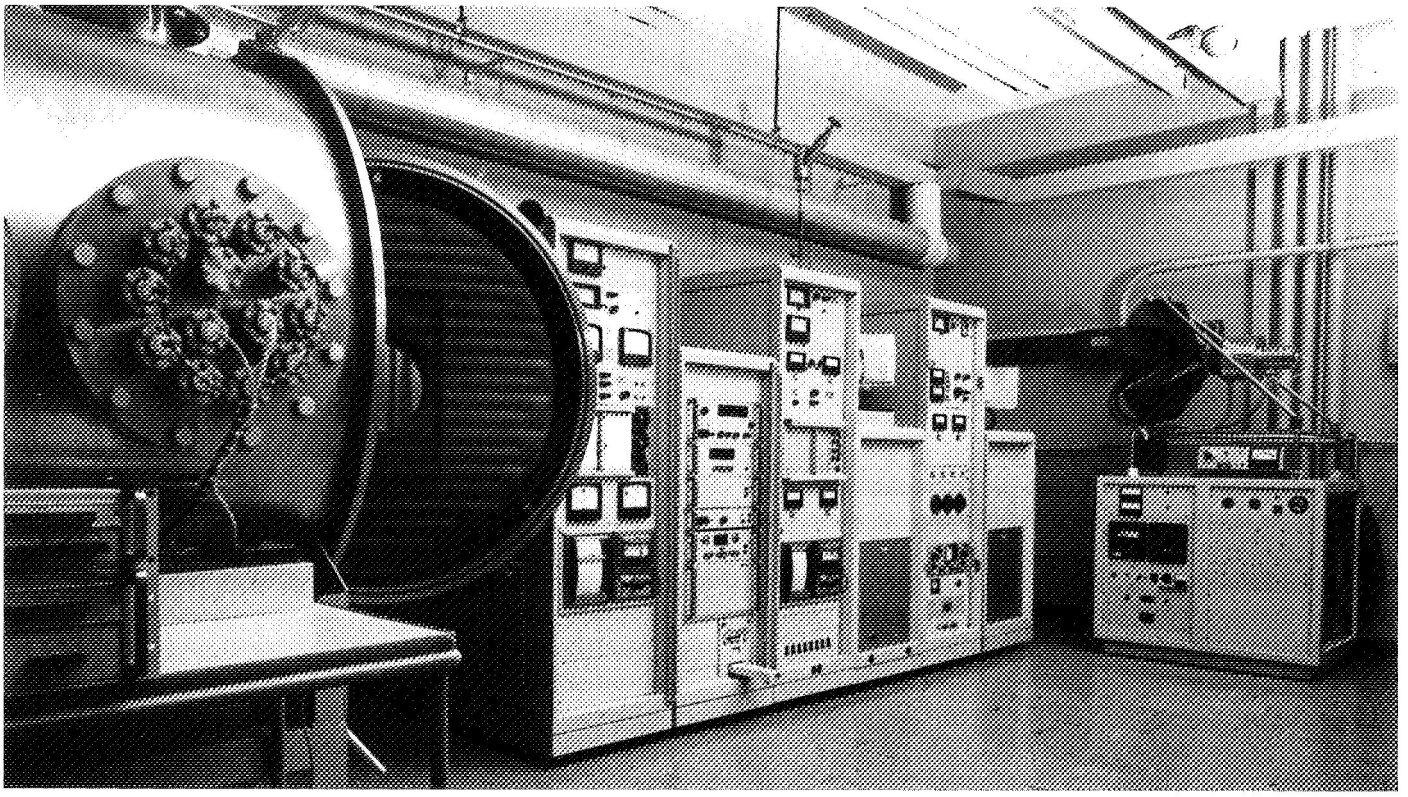

Fig. 6. Generator test laboratory

and monitored and has demonstrated the capability of uninterrupted operation at a pressure of 5×10^{-8} torr for more than a year with a minimum of routine maintenance.

VIII. Results of the Generator Tests

Most of the generators tested at JPL were assembled with lead-telluride materials, employing the 2P-2N or 3P-2N thermoelectric materials.

A. SNAP-11 Generators

The SNAP-11 generators were designed as a possible power source for the *Surveyor* missions. Due to the short mission duration, a short half-life isotope (Cm 242) was selected. To provide a constant hot-junction temperature over the mission duration, the generators were provided with thermal-shutter mechanisms designed to dissipate any thermal energy in excess of that calculated as necessary for the generator operation. The thermoelectric couples used were lead telluride 2P-2N in the early versions and 3P-2N in the improved version. The generator was designed to deliver 30 W at 3.0 V and weighed 30 lb.

The first generator, tested for approximately 3100 h, showed signs of excessive power degradation. The generator was assembled with 2P-2N Pb-Te materials. The degradation was related to a deficiency in the bonding of the elements to the "hot shoes" and to the diffusion of iron from the hot shoes into the *P* elements. In the second unit tested, the *P* leg thermoelectric material was replaced by a Pb-Sn-Te 3P element. The bonding technique was improved, and the pressure holding the elements against the heating capsule was increased. Other secondary problems were also corrected. The generator was extensively tested both in ambient and in a thermal vacuum environment at power input values between 590 and 812 W. Presently it is undergoing long-term life tests. During the thermal vacuum tests, the generator was repeatedly exposed to an environment ranging from $-150°C$ to $+113°C$, corresponding to the estimated lunar environment. During the tests, a constant decrease in the internal argon pressure was observed as a result of slow leakage through the Viton O-ring seals. After the tests, a heavy deposit composed of Au, Cd, Al, and Mg was found on the walls of the chamber (Fig. 7). The generator was also subjected to acceleration and vibration tests to levels up to 18 g (pk) and frequencies of 2500 Hz,

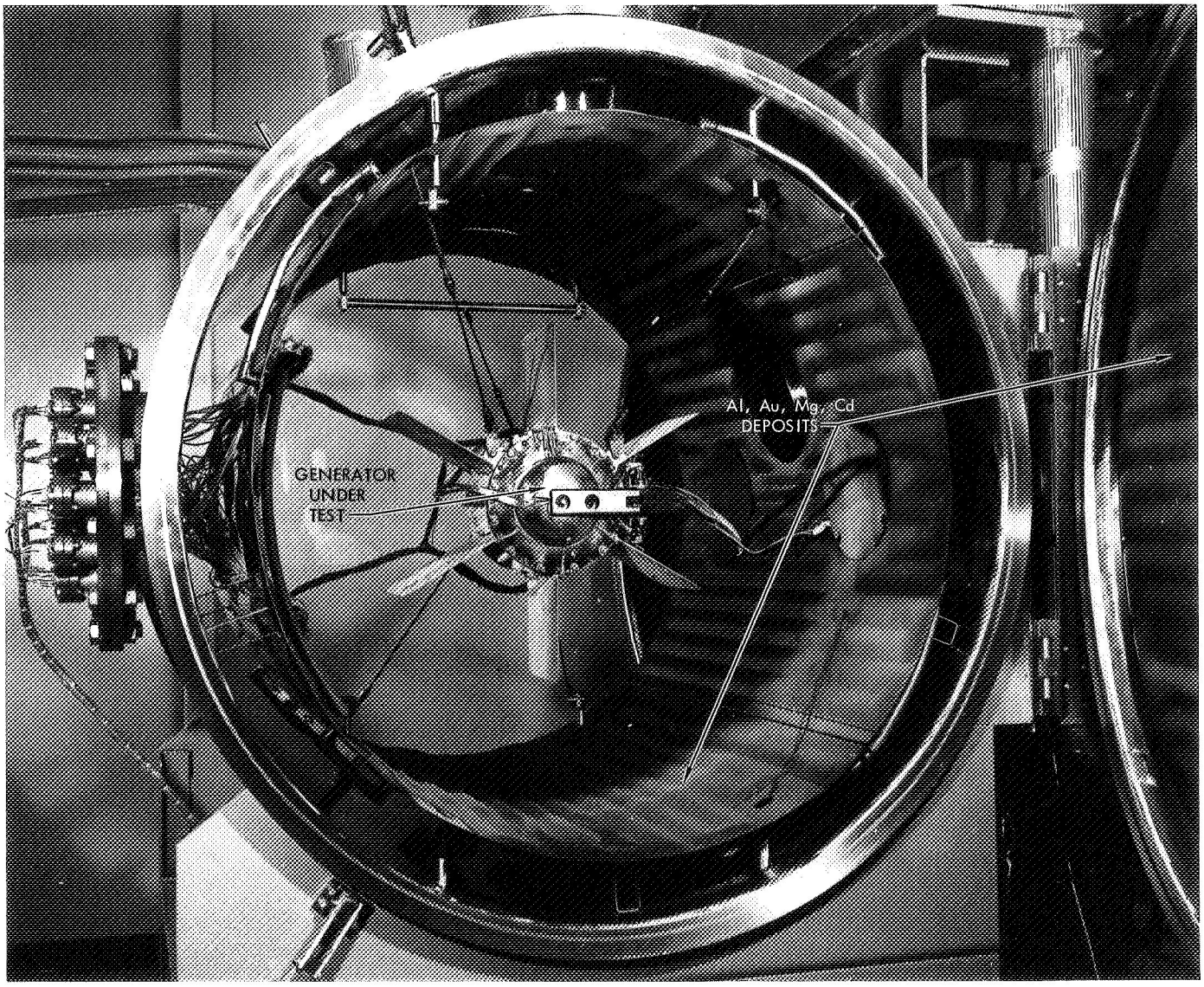

Fig. 7. Generator SNAP-11 in thermal vacuum

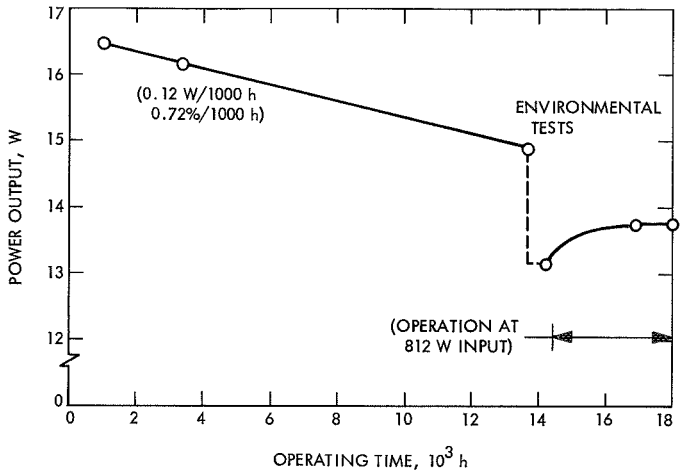

Fig. 8. SNAP-11, power vs time

with 4.5-g, superimposed, white noise. After the tests, an abrupt decrease of 12% in the power output was observed. The power output behavior as a function of time for one value of power input is presented in Fig. 8. Prior to the environmental tests, the average decrease in power output was 0.12 W/1000 h, or 0.72%/1000 h. Since that time (14,000 h), the generator has operated at a power input of 812 W. An increase in power output was observed asymptotically approaching a value corresponding to conditions prior to vibration. It is suspected that metallurgical bonds, which were damaged during the vibration, are slowly healing due to heat and pressure. To date, the generator has operated for over 19,000 h.

B. SNAP-19 Generators

Two SNAP-19 generators were tested at JPL. Generator SN/20 was the engineering prototype of those presently flying on the *Nimbus B-2* spacecraft (Fig. 9), while generator SN/21 was built as an experimental model with modified thermoelectric elements.

Both SNAP-19 generators had the same configuration (Fig. 10), and were assembled with lead-telluride elements. Although generator SN/20 was built with 3P-2N lead-tin-telluride, generator SN/21 used the more common 2P-2N Pb-Te elements but capped with cups (Fig. 11) to provide an improvement in the bonding of the thermo-elements to the hot shoes and to reduce the rate of sublimation.

Operation of generator SN/21 over more than 11,000 h indicated an average power degradation of 0.33 W/1000 h, or 1.2%/1000 h. The degradation rate was first observed during the initial 3000 h. For the next 3500 h, the generator was maintained at 570 W input; however, no data were recorded. Although the generator input was increased to 630 W beyond this point, little degradation was observed over the next 1500 h. At about 8000 h of operation, the generator power output began to decrease again at an average rate of 0.33/1000 h (Fig. 12). Comparison of these results with the degradation rates of other SNAP-19 generators assembled with 2P-2N materials but without cups indicates that in the latter case the average power-degradation rate was approximately 1 W/1000 h, or 3 times higher.

Generator SN/21 was also subjected to magnetic-moment measurements. The magnetic moments were measured at 1 meter from the generator. The results are summarized in Table 5. Although the magnetic effects were partially due to the heater block (carbon steel) and to some other magnetic components included in the construction of this particular generator, it was concluded that most of the magnetic moments were introduced by the 12-A current circulating in the generator. The use of proper intermodule connection and of bucking coils, in conjunction with the suppression of magnetic materials in the generator, would significantly reduce the magnetic field. The tests also indicated that antimagnetic precautions should be taken in the conduction of the power from the generator. The use of coaxial cables is suggested for that purpose.

Table 5. Magnetic moment, SNAP-19 generator 21[a]

Test condition	Dipole moment, γm^3	Maximum radial field at 3 ft, γ
As received, 12-A current	32	80
40-g deperm, 12-A current	31	80
25-Γ exposure, z axis (12-A)	48	135
y axis (12-A)	47	130
x axis (12-A)	42	115
Second 40-g deperm (12-A)	31	80
Power reduced to 6 A	20	50
De-energized	9	22
Third 40-g deperm	7	17

[a]Approximately ⅓ of the moment is attributable to hard ferromagnetic materials in the device. The remaining is proportional to current flow. A total of 3 γm^3 is due to twisted supply cable.

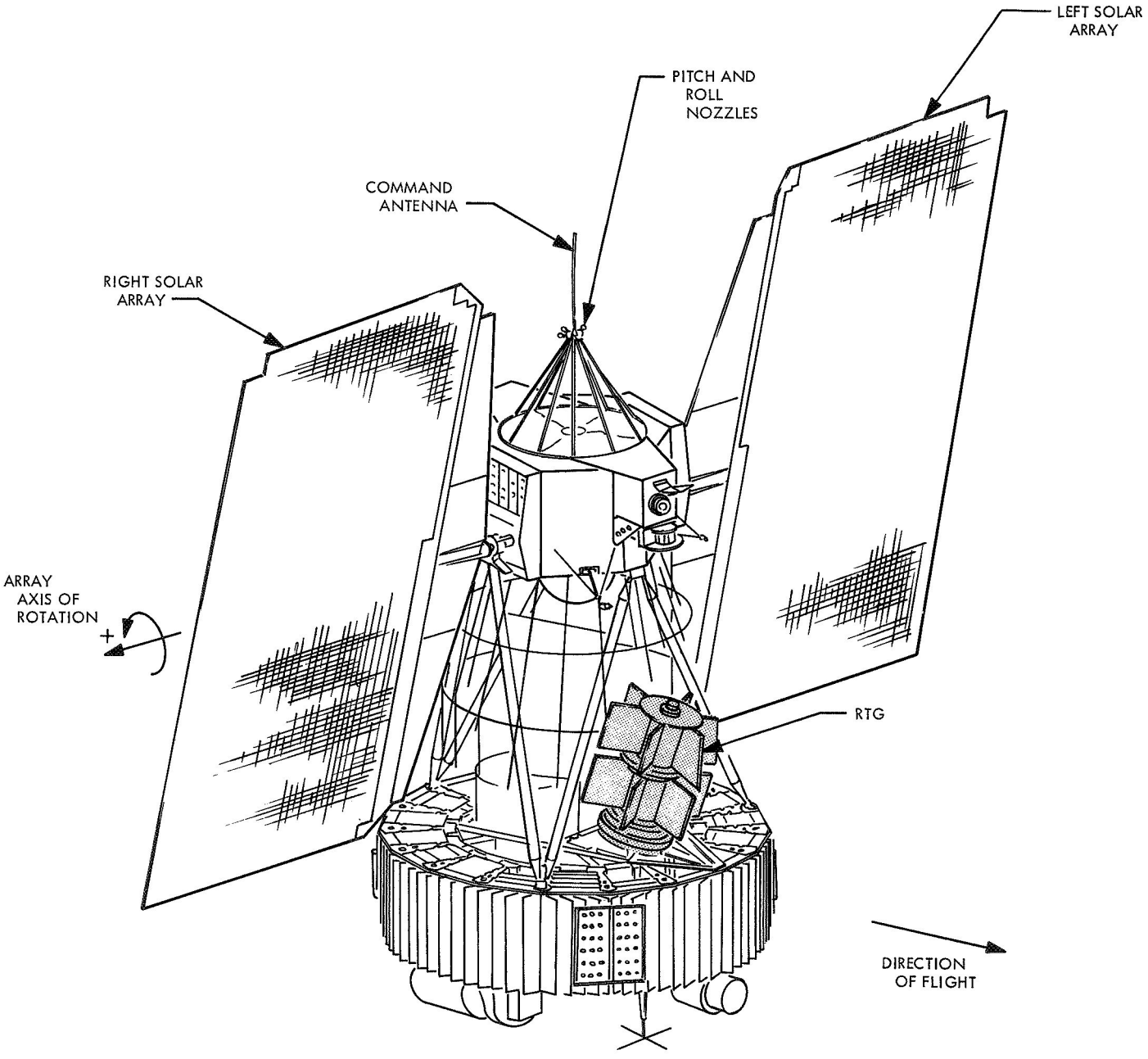

Fig. 9. *Nimbus* spacecraft

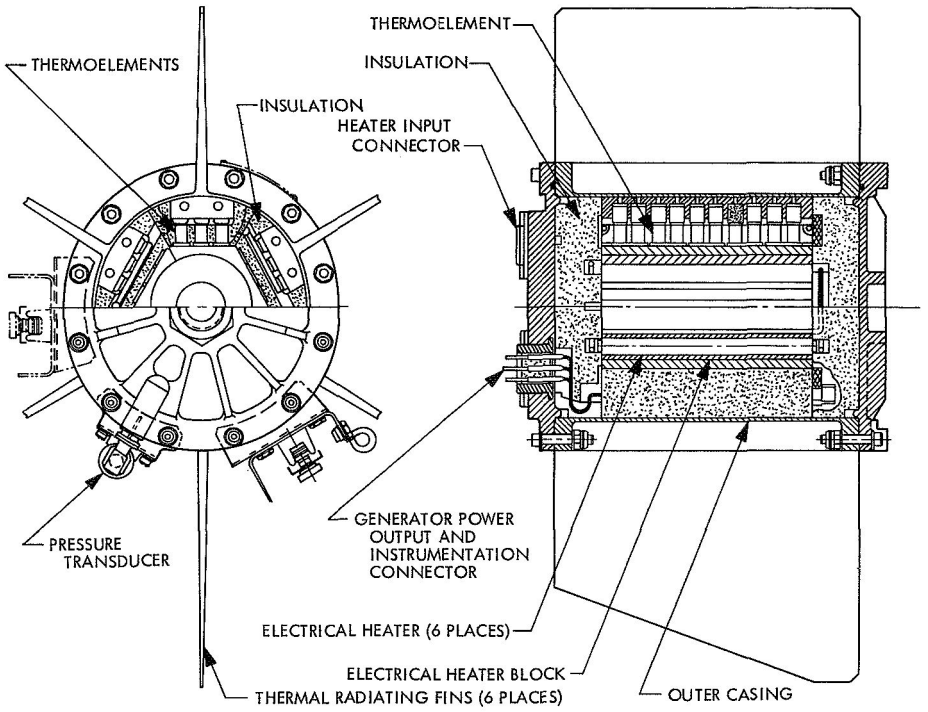

Fig. 10. SNAP-19, section view

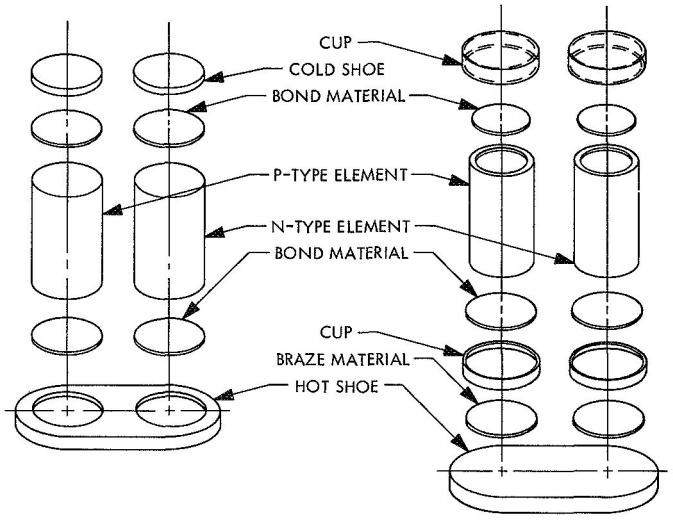

Fig. 11. Pb-Te couples, exploded view

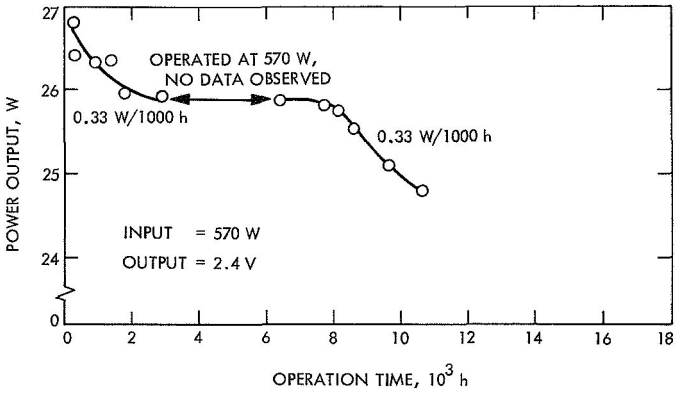

Fig. 12. SNAP-19, SN/21, power vs time

Generator SN/20 was subjected to a much more extensive and demanding test program. After the performance of the normal parametric evaluation in both ambient and thermal vacuum environments at several levels of power input (Fig. 13), the generator was subjected to extensive experiments simulating the in-flight conditions of solar exposure and occultation, and to the investigation of the generator's behavior during the pre-launch period. During the latter phase, the spacecraft, enclosed in the fairing shroud, is cooled by air conditioning. To evaluate this condition, tests were performed which varied the radiator fin-root temperature from +75 to +185°C by varying the thermal shroud temperature in the thermal vacuum facility. The results are presented in Fig. 14. The simulation of solar exposure and occultation was again achieved by varying the fin root temperature between +154 and +185°C. The values selected were based

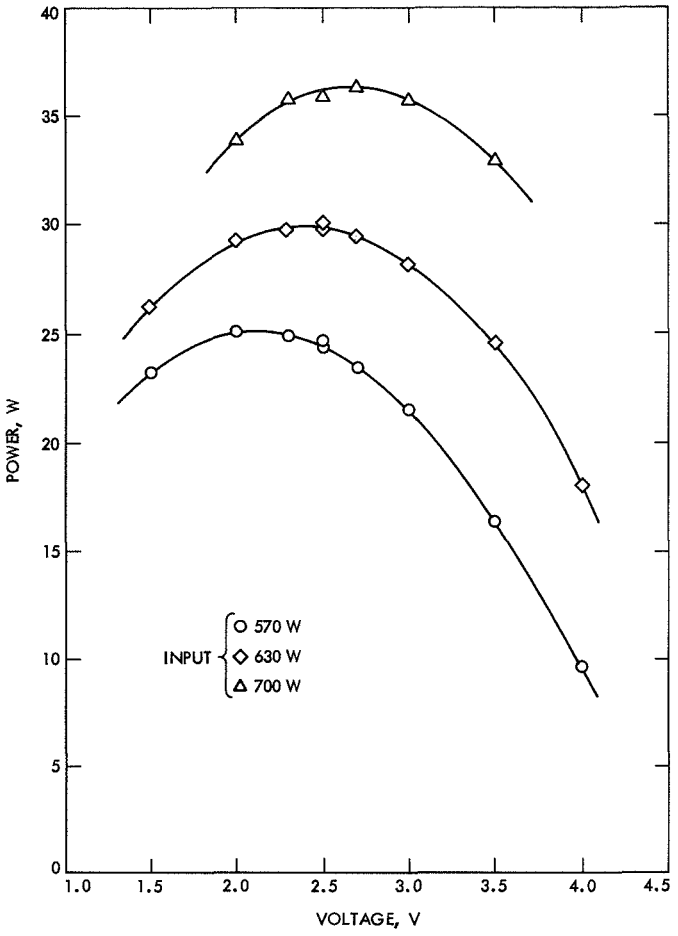

Fig. 13. SNAP-19, SN/20, I-V characteristics

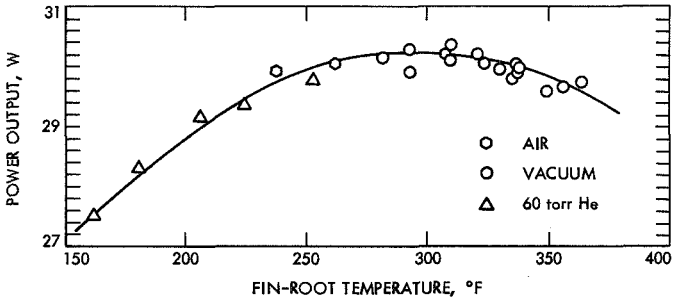

Fig. 14. Fin root/power output dependence

on preflight thermal analysis. The results are presented in Fig. 15. Flight data from *Nimbus B2* indicate that the actual temperature variation is only about 10°C. To evaluate the effects of a different fuel-loading inventory, the generator was tested at several values of input power for a fixed value of output voltage. The results are presented in Fig. 16. At present, the generator is undergoing long-term life tests.

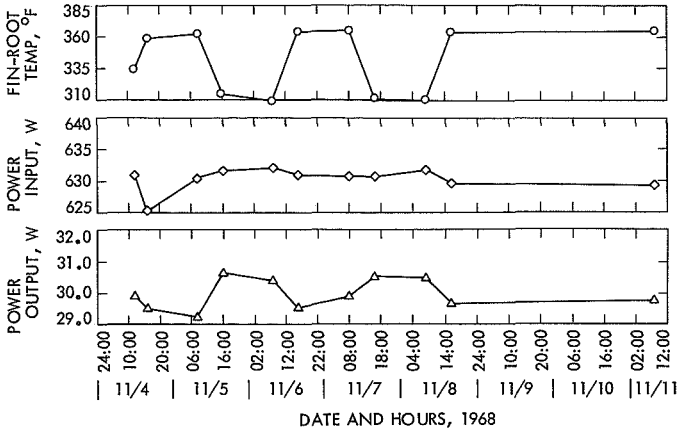

Fig. 15. SNAP-19, SN/20, cycling tests

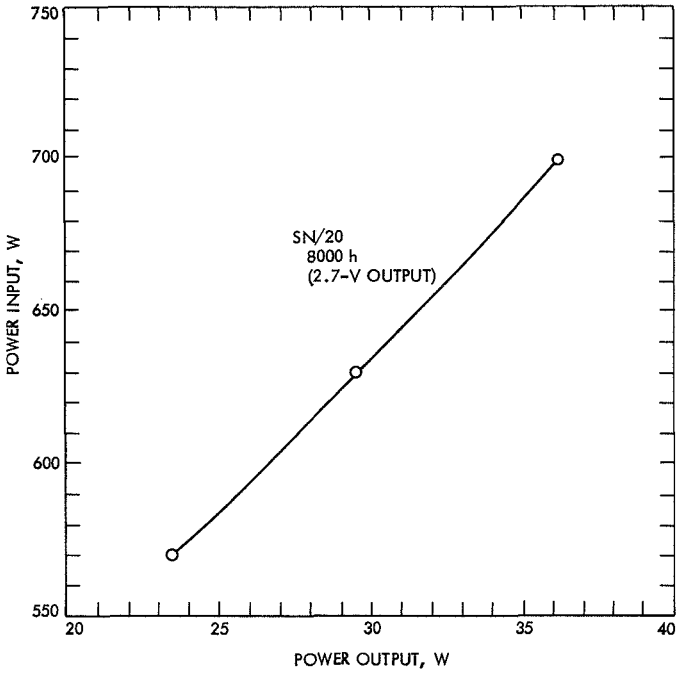

Fig. 16. Power input/power output

The behavior of the generator vs time is presented in Fig. 17 which indicates an average degradation in the generator performance of 0.178 W/1000 h or 0.69%/1000 h over 18,000 h. This low rate of degradation is similar to that observed in the SNAP-11 generator, also built with 3P material. However, it is expected that as a result of the decrease in the pressure of the cover gas due to permeation through the Viton O-ring seals, and the observed progressive increase of the hot junction temperature, the degradation rate of this generator will eventually increase. The degradation mechanisms will probably shift from changes in the thermoelectric material properties to

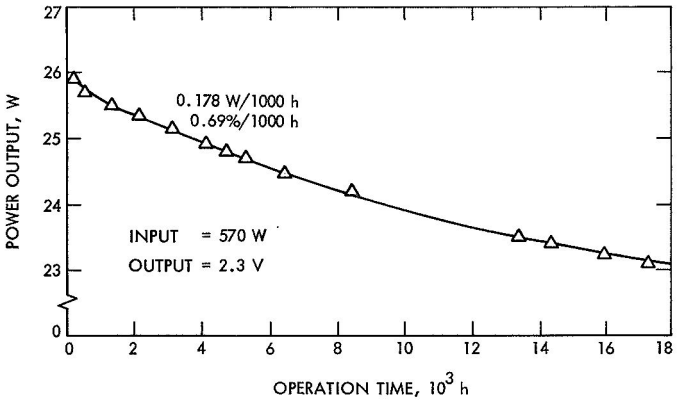

Fig. 17. SNAP-19, SN/20, power vs time

a sublimation phenomena of the thermoelectric elements operating at high temperatures and low cover gas pressure.

C. Integrated Heat-Pipe Tubular Module

A novel design of a thermoelectric generator was tested at JPL (Fig. 18). The device includes a thermoelectric cylindrical module mounted on a stainless-steel heat pipe, employing sodium as the working fluid. The pipe is used as a thermal transfer medium to couple the heat source to the hot junction surface. The excess heat is dissipated by an experimental unidirectional radiator with surfaces of different emissivities. The tubular module is composed of flat discs of 2P-2N lead-telluride thermoelectric material, separated by mica insulator, and hermetically sealed into a tubular module. The construction of the module is schematically presented in Fig. 19. The concept is the first step toward a fully "cascaded" thermoelectric generator combining SiGe with PbTe. Efficiencies in the order of 7% are expected with such a combination.

The test of the tubular-module generator confirmed the feasibility of the design. Figure 20 presents the temperature-profile distribution within the device. It was successfully tested for 1978 h. However, after the generator was subjected to several thermal shocks, its performance decreased by 54% of the original value. Metallographic examinations revealed deficiencies which resulted in partial internal short circuits. An improved model, in which the original deficiency has been corrected, will be incorporated in the construction of the cascaded generator.

D. SNAP-27 Generators

Testing was initiated on a SNAP-27 generator, mod 15, similar to the one to be deposited on the moon to power

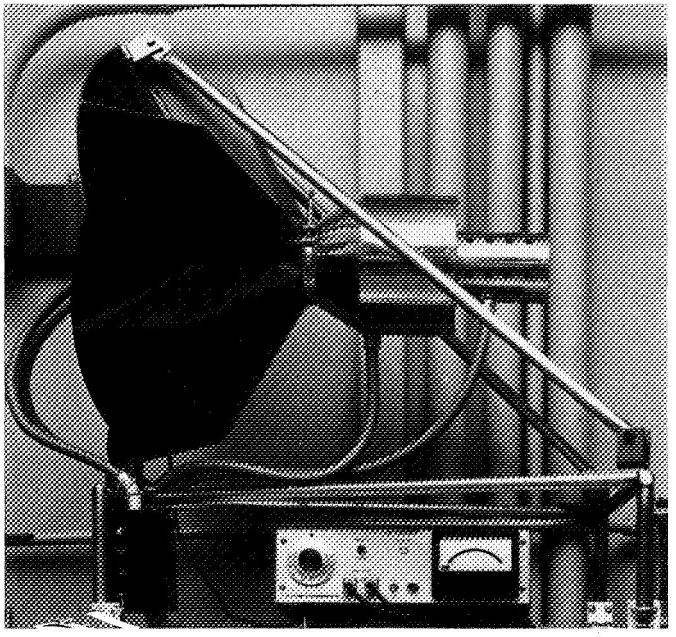

Fig. 18. Tubular thermoelectric generator

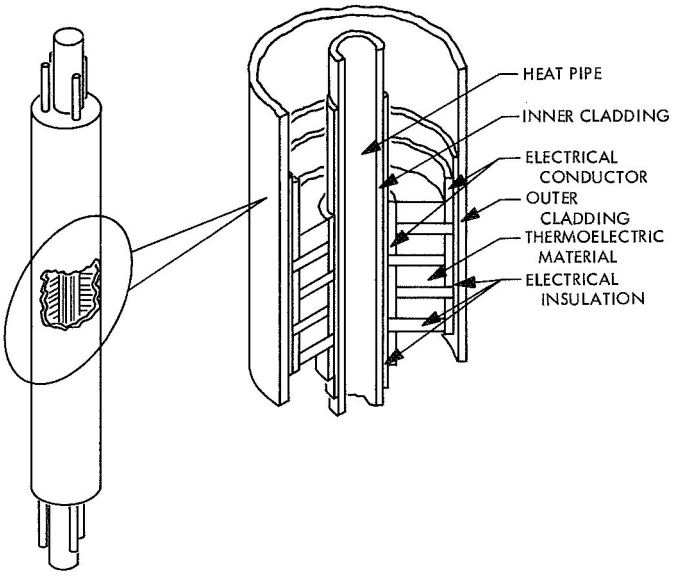

Fig. 19. Tubular module, exploded view

the ALSEP experiment. The objective of the test is to evaluate the performance of the generator and its long term behavior, to project its possible application to other space missions, and to support the evaluation of the generator during the mission. SNAP-27 weighs 21.5 kg, it is assembled with 3P-3N thermoelectric lead-tin-telluride materials, and is designed to deliver 16 V at its output. Figure 21 shows the generator being readied for test. The generator was tested at three levels of power input: 1500,

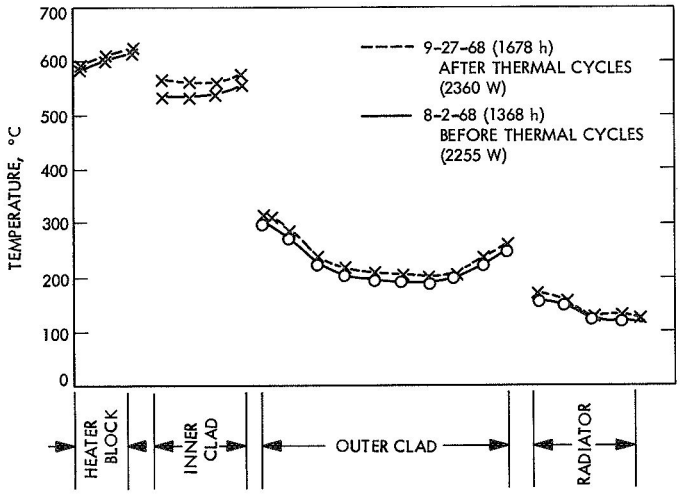

Fig. 20. Tubular module temperature profile

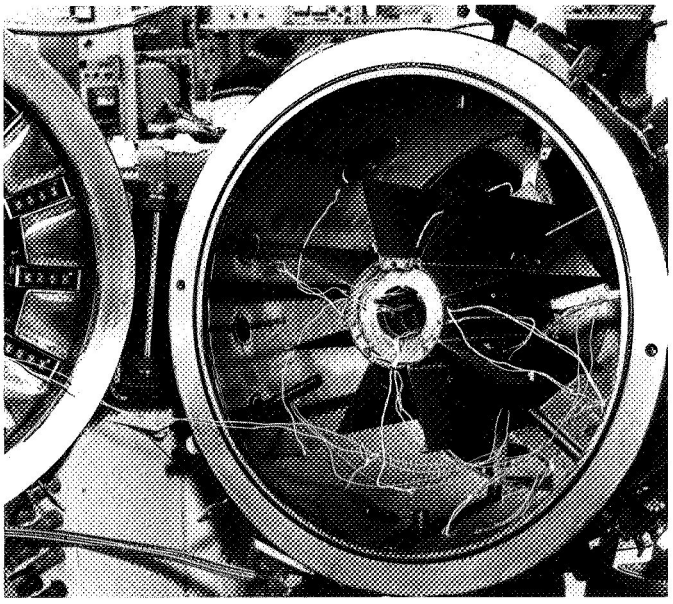

Fig. 21. SNAP-27 in test chamber

1450, and 1400 W and at a lower power input point used as a reference for start-up. Figure 22 shows the SNAP-27 generator performance during these tests. During the life testing the generator is operating at 1500 W input and 16 V output, which corresponds to a hot frame temperature of 560°C. At these conditions the generator is delivering a power output of 74.5 W. At present the generator has operated 4000 h under these conditions, without apparent degradation in output power.

E. Module Tests

The most relevant test results of multielement modules are summarized in Fig. 23. The results, supported by

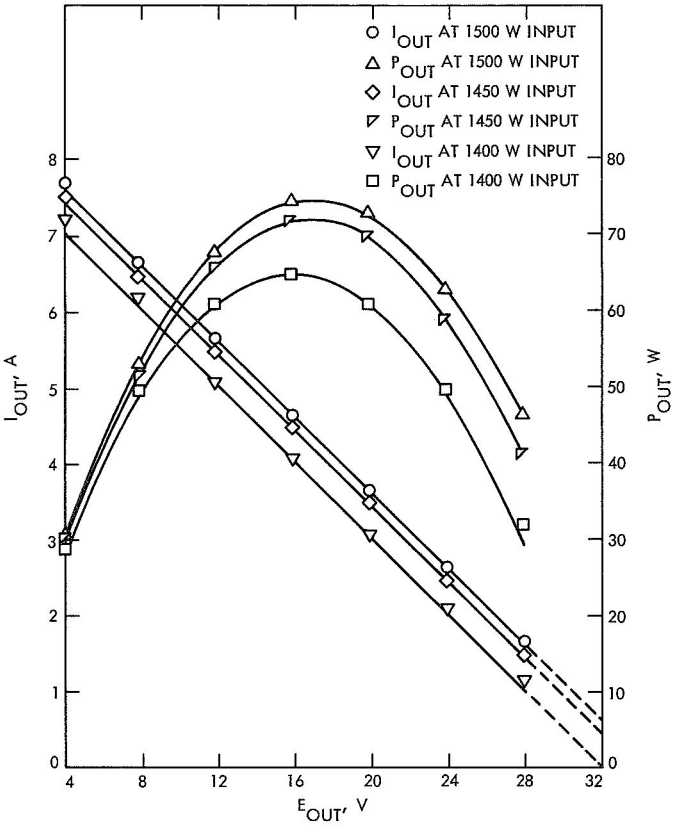

Fig. 22. SNAP-27 generator performance

3,290,000 coupled hours, confirm the fact that units assembled with 3P-2N or 3P-3N thermoelectric materials degrade at an average rate of 0.7%/1000 h. These results were obtained from the tests of multielement modules and of the SNAP-11 and SNAP-19 generators for periods of time between 14,000 and 20,000 h.

IX. Conclusions

The Jet Propulsion Laboratory, under the sponsorship of NASA, has developed a very extensive program with the purpose of testing and evaluating radioisotope thermoelectric generators and performing the necessary spacecraft integration studies for future flight missions. The study of the problems of integrating the RTG with the scientific instrumentation has been approached in both a theoretical manner, with the use of computer programs, and by experimental verification, using real fueled capsules and flight-type instruments. The testing of several generators for an approximate accumulated time of more than 60,000 h, and of multicouple modules for a total of more than 70,000 h, has demonstrated the feasi-

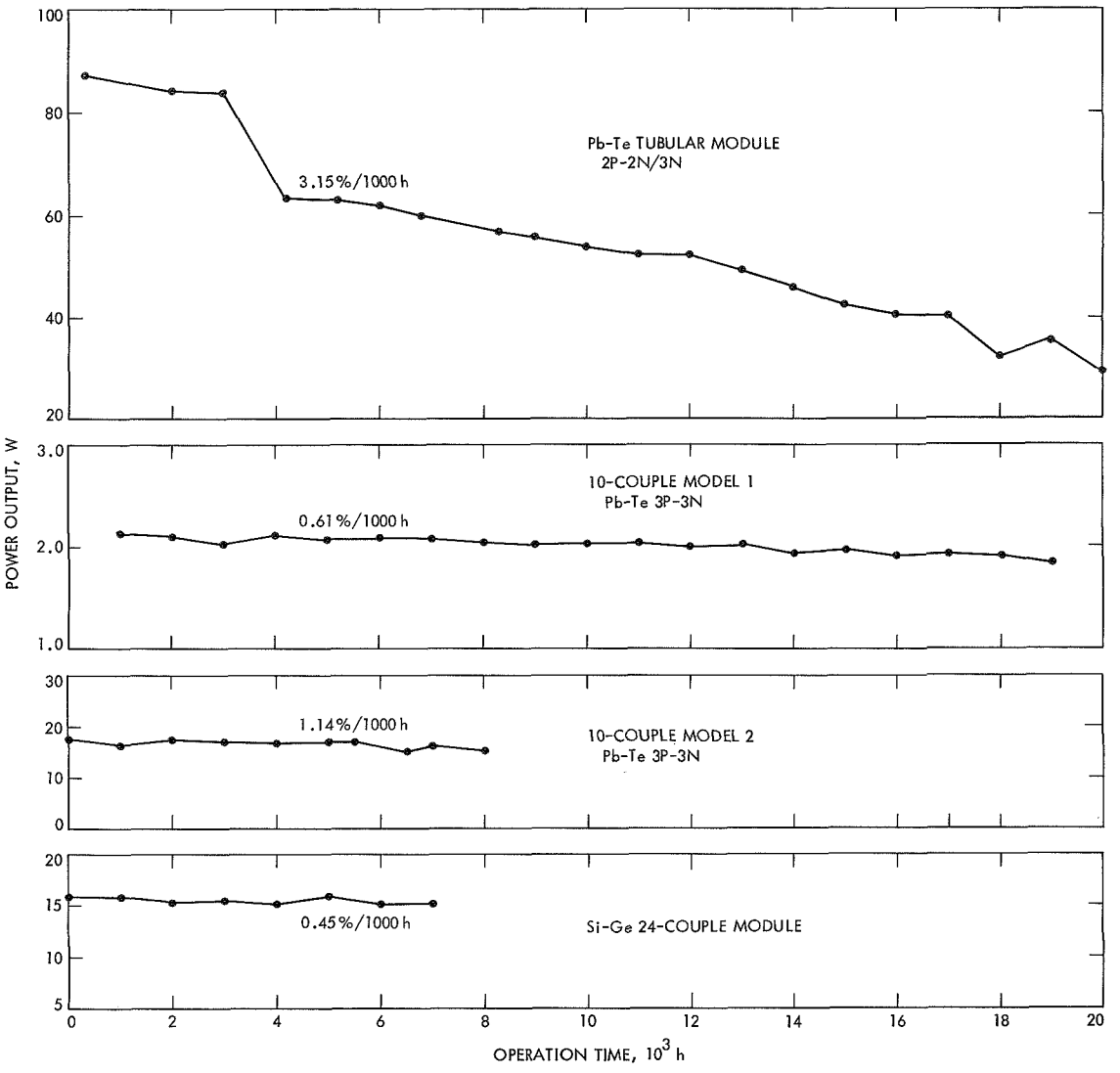

Fig. 23. Multielement modules, power vs time

bility of the use of RTGs in long-term flight missions. The use of automatic test equipment and data recording processes has resulted in effective manpower savings and has minimized the possibility of operator error. The long-term tests of two generators and of several modules assembled with 3P and 2N or 3N Pb-Te thermoelectric materials confirmed that this material combination degrades at a rate of 0.7%/1000 h.

NASA — JPL — Coml., L.A., Calif.

N71-16726

TECHNICAL REPORT STANDARD TITLE PAGE

1. Report No. 32-1495	2. Government Accession No.	3. Recipient's Catalog No.
4. Title and Subtitle THERMOELECTRIC GENERATORS FOR DEEP SPACE APPLICATION		5. Report Date January 15, 1971 6. Performing Organization Code
7. Author(s) P. Rouklove, V. Truscello		8. Performing Organization Report No.
9. Performing Organization Name and Address JET PROPULSION LABORATORY California Institute of Technology 4800 Oak Grove Drive Pasadena, California 91103		10. Work Unit No. 11. Contract or Grant No. NAS 7-100 13. Type of Report and Period Covered Technical Report
12. Sponsoring Agency Name and Address NATIONAL AERONAUTICS AND SPACE ADMINISTRATION Washington, D.C. 20546		14. Sponsoring Agency Code

15. Supplementary Notes

16. Abstract

To provide a source of electrical energy independent of the sun, for the use of unmanned spacecraft investigation of the outer planets, the Jet Propulsion Laboratory (JPL) is evaluating radioisotope thermoelectric generators. Criteria for the selection of the thermoelectric materials, the design of the generator, and its integration with the spacecraft are discussed. Results of the tests of 10 generators that have been, or are presently, under test at JPL are also presented.

17. Key Words (Selected by Author(s))	18. Distribution Statement
Interplanetary Spacecraft, Advanced Power Sources Thermoelectric Outer-Planet Spacecraft (TOPS) Project	Unclassified -- Unlimited

19. Security Classif. (of this report)	20. Security Classif. (of this page)	21. No. of Pages	22. Price
Unclassified	Unclassified	20	

HOW TO FILL OUT THE TECHNICAL REPORT STANDARD TITLE PAGE

Make items 1, 4, 5, 9, 12, and 13 agree with the corresponding information on the report cover. Use all capital letters for title (item 4). Leave items 2, 6, and 14 blank. Complete the remaining items as follows:

3. Recipient's Catalog No. Reserved for use by report recipients.

7. Author(s). Include corresponding information from the report cover. In addition, list the affiliation of an author if it differs from that of the performing organization.

8. Performing Organization Report No. Insert if performing organization wishes to assign this number.

10. Work Unit No. Use the agency-wide code (for example, 923-50-10-06-72), which uniquely identifies the work unit under which the work was authorized. Non-NASA performing organizations will leave this blank.

11. Insert the number of the contract or grant under which the report was prepared.

15. Supplementary Notes. Enter information not included elsewhere but useful, such as: Prepared in cooperation with... Translation of (or by)... Presented at conference of... To be published in...

16. Abstract. Include a brief (not to exceed 200 words) factual summary of the most significant information contained in the report. If possible, the abstract of a classified report should be unclassified. If the report contains a significant bibliography or literature survey, mention it here.

17. Key Words. Insert terms or short phrases selected by the author that identify the principal subjects covered in the report, and that are sufficiently specific and precise to be used for cataloging.

18. Distribution Statement. Enter one of the authorized statements used to denote releasability to the public or a limitation on dissemination for reasons other than security of defense information. Authorized statements are "Unclassified—Unlimited," "U. S. Government and Contractors only," "U. S. Government Agencies only," and "NASA and NASA Contractors only."

19. Security Classification (of report). NOTE: Reports carrying a security classification will require additional markings giving security and downgrading information as specified by the Security Requirements Checklist and the DoD Industrial Security Manual (DoD 5220.22-M).

20. Security Classification (of this page). NOTE: Because this page may be used in preparing announcements, bibliographies, and data banks, it should be unclassified if possible. If a classification is required, indicate separately the classification of the title and the abstract by following these items with either "(U)" for unclassified, or "(C)" or "(S)" as applicable for classified items.

21. No. of Pages. Insert the number of pages.

22. Price. Insert the price set by the Clearinghouse for Federal Scientific and Technical Information or the Government Printing Office, if known.